Journal of Nuclear Materials 390–391 (2009) 76–79

Contents lists available at ScienceDirect

Journal of Nuclear Materials

journal homepage: www.elsevier.com/locate/jnucmat

Studies of hydrocarbon cracking by molecular beam injection in He plasmas in the TJ-II stellarator

F.L. Tabarés *, D. Tafalla, T.G. Wurgie, J.A. Ferreira

Laboratorio Nacional de Fusión, Asociación EURATOM/Ciemat, 28040 Madrid, Spain

ARTICLE INFO

PACS:
52.70.Kz
52.40.Hf
52.25.Vy
52.55.Fa
33.20.Lg

ABSTRACT

Hydrocarbons (CH_4 and C_2H_4) have been injected in TJ-II He plasmas by means of the supersonic helium beam set-up typically used for the edge characterization in hydrogen plasmas. The radial profiles of the emission of the CH(A-X) band and $H\alpha$ were recorded along the hydrocarbon penetration. For all cases, the emission profiles of the recorder species can be fitted to a simple model with one single parameter, related to the velocity along the observation line of the CH and H radicals resulting from the initial cracking of the hydrocarbon. A H_2 beam was also used for reference of velocity distribution. The penetration of H atoms, which emit $H\alpha$, is in the case of hydrocarbon cracking twice as large as in H_2 dissociation, depending on hydrocarbon. A similar radial profile of the CH radicals was found for both hydrocarbons, thus suggesting the existence of a common precursor. The ratio of $H\alpha$/CH(A-X) photon emissions for the two hydrocarbons investigated is compatible with a reaction stoichiometry yielding 3 H atoms per CH.

1. Introduction

The transport of sputtered carbon (either by physical or chemical processes) in a plasma is paramount in the assessment of codeposit formation, with significant tritium content, on the elements surrounding the plasma of a carbon-based fusion device, as foreseen for the initial phase of ITER. Several transport codes have been developed for this purpose [1,2], but the direct input of the relevant kinetic rates still has a crucial impact on the predictions. For the case of chemical sputtering, one of the parameters which can strongly affect the location where the first generation of carbon ions is launched, and hence their toroidal and poloidal spreading along field lines, is the velocity at which their precursors are created form the cracking of the hydrocarbons produced. Due to the complexity of process, with many possible neutral and ionic fragments as intermediates (summarized in the HYDKIN database [3]), direct measurements of this important parameter are of especial relevance. However, the present available direct information about the break-up in fusion plasmas is incomplete and, in many cases, the perturbative characteristics of the reported experiments cannot be completely ruled-out. Instead of molecular fragments, atomic carbon has been often preferred for velocity measurements, thus preventing direct discrimination between the physical or chemical origin of this impurity. So, the toroidal dispersal of C atoms from methane injection in DITE yielded energies for the break-up chain of that hydrocarbon of 0.1–1 eV [4]. This is a typical values presently used for the simulations in devoted codes. Similarly, a value of $E_C = 3$ eV was deduced from the velocity distribution broadening for chemically sputtered carbon in L mode plasmas in DIII-D [5], whereas values of $E_C \sim 0.6$ eV were recently reported for methane injection in the divertor of that device [6]. On the other side, very little information is available to the author's knowledge on the kinetic energy of ejected H atoms during hydrocarbon cracking. In the present work we report the first measurements of molecular beam injection of hydrocarbon species aimed to provide direct information in this important topic. Contrary to simple puffing through the limiter, as done before [7,8], molecular beam injection benefits from the low divergence (<1.5° in our case) and monoenergetic characteristics (speed ratio > 10) of this type of source. The high localization of the injection point together with its pulsed characteristics allows for good signal to noise discrimination under non-perturbative, low fluence conditions. In addition, the excellent recycling control achieve by litiumization of TJ-II in the last campaign [9] prevented the after shot increase of the recorded emission lines. Moreover, the use of He background plasmas enables direct focusing on electron-driven processes alone.

2. Experimental set-up

The set-up used for the injection is the same as that routinely used for the edge parameter characterization in TJ-II. This is a supersonic He beam, operated in a pulse mode (pulse length

---

* Corresponding author.
E-mail address: tabares@ciemat.es (F.L. Tabarés).

0022-3115/$ - see front matter © 2009 Elsevier B.V. All rights reserved.
doi:10.1016/j.jnucmat.2009.01.077

0.5–2 ms, repetition frequency <200 Hz) located in a top window of the main chamber. Details about operation of the diagnostic as a He beam can be found elsewhere [10]. The edge parameters for the experiments here reported are given in Fig. 2. Although they correspond to density-matched H plasmas, edge parameters were very similar for all the ECRH He background plasmas, as deduced from the neutral Li beam and Langmuir probe data [11]. The two hydrocarbons, methane and ethylene, were fed through the beam into the plasma edge. Low stagnation pressures (1.0–1.5 Bar) were used in order to prevent possible perturbations of the edge parameters and the formation of clusters in the beam, and local densities of injected species were kept below a 1% of the corresponding electron density. Both aspects were experimentally verified. Respect to the second point, time of flight measurements were carried out by a mass spectrometer locate at 2.5 m opposite to the beam. This allowed for the determination of the velocity of the injected species. The information so obtained was used to define the time of arrival of the beam to the observation region. Thus an exact onset of the emission intensity associated to the beam was identified, allowing for a good discrimination against plasma emission fluctuations. An example of this can be found in Fig. 1. Interference filters at 431 nm (FWHM 1 nm) and Hα (FWHM 10 nm) were coupled to the standard detection system of the beam. Note that for the CH emission, the head of the A-X band (Q, $v = 0–0$ line) is located at 431.5 nm, so that less than a ~30% of the total vibro-rotational emission spectrum of the CH emission, (assuming a $T_{rotr} = 3500$ K) is recorded [7]. The detection volume was selected in order to cover the ~3 cm full width of the beam at the location of the array (1.2 m from the beam source). Signals were digitized at 10 kHz on a PCI card in a PC and transferred to the main Data Acquisition System of TJ-II. The signal of the valve voltage was used for time reference. The peak intensity was used for the profile reconstruction when good discrimination over the plasma background was possible. Otherwise, an algorithm was developed in order to subtract the fluctuating background at the measuring time, between the arrival of the beam and the end of the pulse.

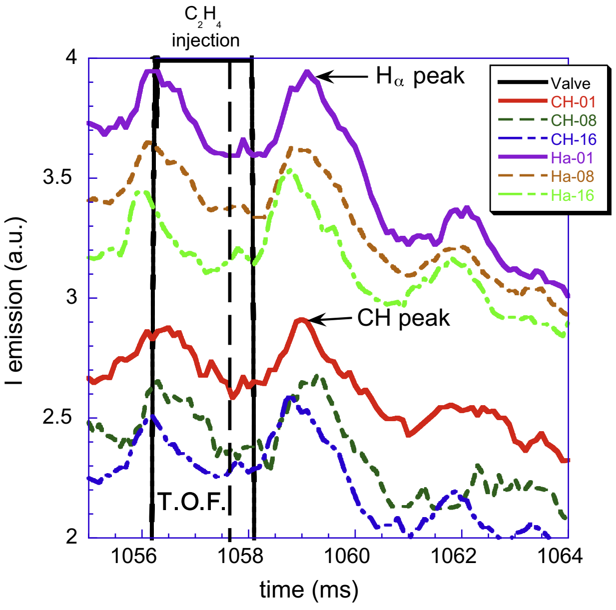

Fig. 1. Time traces of Hα and CH emission signals at three different radial locations upon injection of ethylene in a He plasma. Vertical bars: pulse of the beam valve. Note the delay of ~2.7 ms in the peak maximum associated to the TOF of the ethylene pulse (peak onset at 1.6 ms). The shadowed area corresponds to the integration time.

3. Results

In Fig. 3, the profile of Hα emission from three different sources is displayed. From left to right, the source was molecular hydrogen, methane and ethylene, respectively. The location of the nominal LCFS is given in Fig. 2, and corresponds to $x = 3$ cm in Figs. 3 and 4. As seen, the emission maximum for H_2 injection is located further outside the plasma as compared to the maxima from hydrocarbon injection, thus suggesting a lower velocity for the H atom generated by molecular cracking of hydrogen. Simultaneously, the CH emission profile was also recorded, and the results are displayed in Fig. 4. Very similar shapes are seen for the profiles regardless of the injected species. Since the ionization rate of CH radicals is significantly larger than that for H at the edge temperatures here involved (see Table 1), one can conclude that CH is launched into the plasmas at higher velocity than H atoms. This simple observation is in obvious contradiction with a common precursor for both species, since a factor 13 higher for H would be expected by simple momentum conservation constrains for a Frank–Condon type (adiabatic) dissociation of a common precursor. In order to get some quantitative insight from the experimental profiles, fittings to the experimental data are also shown in Fig. 3 and 4. These fittings correspond to a functionality of the form

$$I(x) = A \cdot x \cdot \exp(-b \cdot x^2), \tag{1}$$

where x is the distance from the point where the species is injected into the plasma along the detection axis, $I(x)$ stands for the emission intensity at x and A is a proportionality factor. For the simplest case of a molecular beam of the recorded radicals propagating into a linear density profile, $ne(x) = n(a) + m \cdot x$, with velocity v, the value of the exponential constant would be given by $b = \langle\sigma v\rangle_{iz} \cdot m/2 \cdot v$, where $\langle\sigma v\rangle_{iz}$ stands for the effective ionization rate constant of

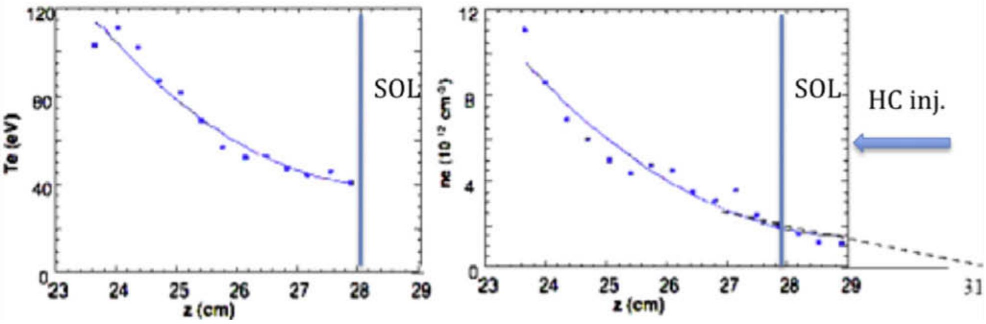

Fig. 2. Radial profiles of the edge parameters prevailing during the injection experiments in equivalent H plasma. Linear extrapolation up to $z = 31$ cm is shown. The location of the LCFS is at $z = 28$ cm.

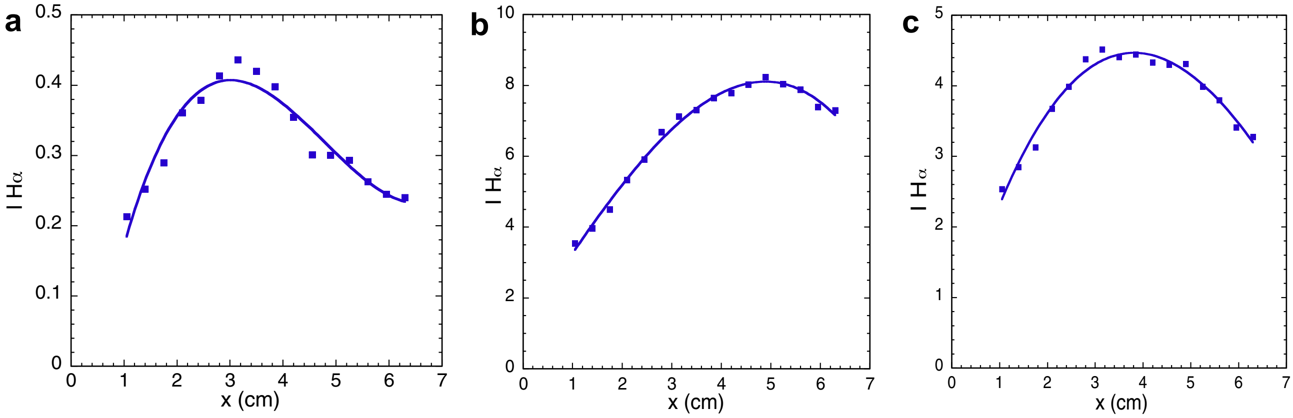

Fig. 3. Profile of line-corrected Hα emission (a.u.) during the injection in a He plasma of: (a) H_2, (b) CH_4 and (c) C_2H_4.

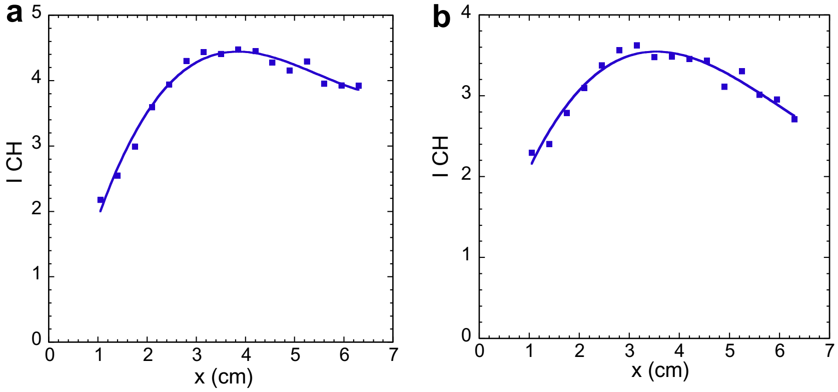

Fig. 4. Profile of line-corrected CH emission (a.u.) during the injection in a He plasma of: (a) CH_4 and (b) C_2H_4.

the corresponding radical by electron impact and the ratio of excitation/ionization events is assumed constant within the detection region. For the linearized density profile shown in Fig. 2, with $m = 10^{12}$ cm^{-3}/cm, the *b* values so obtained are shown in Table 2 for all the cases analyzed. As seen, good fitting to the data is generally obtained with the simple expression given in 1. The velocity values that would be deduced from the fittings to the simplified model are given in the figures and summarized in Table 2. Also shown in the table are the velocity values deduced from the experimental profiles if the excited radicals were homogenously distributed into the plasma volume observed by the corresponding lines of sight (LOS), i.e., normalizing the recorded intensities to the length of the corresponding chords. As expected, lower velocities are deduced under this assumption. Changes in the density profile into the SOL, such as an exponentially decaying density beyond the LCFS, were also tried, and velocities systematically lower by only a 10–15% were deduced in that case.

From the relative intensities of Hα and CH and the corresponding gains of the detectors, a value of Hα/CH ~ 20 was obtained for both hydrocarbons for the filter widths used here. However, as stated above, only a fraction of the A-X band for CH is recorded by the interference filter (mainly the Q branch), so that a H/CH photon ratio of the corresponding emitted signals is actually ~5. Assuming a typical *S/X* factor of 15 for Hα emission and a *D/XB* value of 27 for CH emission from methane cracking [7], one has

$$\frac{I(\mathrm{H}\alpha)}{I(\mathrm{CH})} = 5 = n\frac{[\mathrm{H}]}{[\mathrm{CH_4}]}\cdot\frac{D/XB_{\mathrm{CH}}}{S/XB_{\mathrm{H}\alpha}} \approx 2\cdot n\frac{[\mathrm{H}]}{[\mathrm{CH_4}]}. \tag{2}$$

Therefore, a ratio of $n \sim 2.5$ H atoms per injected methane seems to be produced during the molecular break-up. Even when these values are obviously only approximated, the resulting H/CH_4 ratio is quite close to the stoichiometry resulting in: $CH_4 + e \rightarrow CH + 3H$. Interestingly, the same H/molecule ratio seems to hold for the two hydrocarbon species here tested.

4. Discussion and conclusions

The injection of hydrocarbons into the plasma periphery has been used since long for the determination of the photon/molecule ratio, *XB/D*, critically required for the estimates of the chemical

Table 1
Expected penetration of injected molecules into the plasma edge.

Injected species	H_2	CH_4	C_2H_4
TOF velocity (10^5 cm/s)	1.6	0.6	0.43
Total ion. + dissociation rate constant @40 eV in cm^3 s^{-1} from [3]	0.6×10^{-7}	1.5×10^{-7}	2.8×10^{-7}
Penetration depth in plasma (cm)	1	0.13	0.05

Table 2
Summary of the fitting parameters in Figs. 3 and 4 and deduced velocities according to the simplified models described in the text.

Injected species	H_2	CH_4	C_2H_4	CH_4	C_2H_4
Detected radical	H	H	H	CH	CH
b (10^{-2} cm^{-2})	7	3.5	5	5.5	5.5
v (10^5 cm/s)$_{\text{model MB}}$	3.3	6.7	4.3	11.4	10
v (10^5 cm/s)$_{\text{model LOS}}$	2.1	4.2	3.0	7.3	6.1

sputtering yields in carbon-based PFC devices [7]. Some of these experiments have also addressed the dynamics of the cracking process by fitting the recorded emission profiles to existing impurity transport models, as ERO or DIVIM [1,2]. Unfortunately, these models require a large number of input parameters, and geometrical or surface effects can override gas phase dynamics, as it is the case for sticking probabilities of the gas phase created radicals [1]. To date, at least to the author's knowledge, no direct recording of the velocity of the radicals here addressed has been reported, and only sub-Doppler spectroscopy of the resulting atomic C, leading to the dispersion of values mentioned in the Introduction, provides indirect information about the dynamics of the hydrocarbon break-up in the plasma. It must be pointed out that, in the experiments here presented, no carbon materials were present in the neighbourhood of the observation region. Also, the pulsed characteristics of the injection allows for a much better discrimination of the possible sources of the observed radiation and for the injection of very low, non-perturbing doses. In that sense, molecular beam injection appears as a powerful technique to address the gas dynamics of the plasma–hydrocarbon interaction. However, the interpretation of the results is still hindered by the potential complexity of the reactive system. This is evident from the data shown in Table 2. So, the velocities deduced for the CH radical would imply very large kinetic energies for this radical, up to 8.5 eV if the MB model is applied for the methane case. This is larger that the total available energy from the ground state dissociation of methyl radicals [3]. One possible explanation for these energetic radicals is the Frank–Condon dissociation from highly excited methyl radicals. Although the presence of such radicals has been postulated from laser photofragmentation studies in molecular beams of methane [12], the data here provided are not free of ambiguity due to lack of information on the full spatial distribution of the detected emission. Thus, the possible contribution to the LOS from molecular species in the SOL undergoing direct formation of excited radicals cannot be rued out. Examples of this are the processes (of large impact in tenuous plasmas [13,14]) $CH_4 + e- \rightarrow CH^* + \text{products}$ or $H_2 + e \rightarrow H\alpha + H$. Studies of the emission profiles in the direction perpendicular to the beam propagation are presently underway to clarify this point. In addition, the formation of excited radicals from ionic precursors, which would be spread along the field lines, could also contribute to the measurements and their presence needs to be rued out. In this direction, Detection of CH^+ fragments by optical emission spectroscopy are also underway.

Even with these caveats in mind, two remarks are worth making concerning the results: First, the origin of the Hα emission from hydrocarbon breaking seems not to be the cracking of molecular hydrogen that could be produced directly during the hydrocarbon fragmentation, as for example $CH_4 + e \rightarrow H_2 + CH_2$. Second, the fact that similar penetration profiles and H/CH photon ratios are seen during the injection of both hydrocarbons suggest the presence of a common precursor, as it could be CH_2, as proposed by other authors [14]. It should be pointed out here that this result is in apparent contradiction with our previous determinations by hydrocarbon puffing through a graphite limiter in TJ-II [15], where the ratio of H/CH emission intensities was 3 times higher for ethylene injection than for methane, thus stressing the need of pure gas phase experiments, as those presented here, for the study of the dissociation dynamics into the plasma. Finally, it should be kept in mind that a high velocity for the carbon source from chemical sputtering processes will lead to a deeper penetration into the plasmas and hence a lower prompt redeposition probability and lower screening of C atoms, as deduced from some dedicated experiments [8,16].

Acknowledgments

This work was partially supported by the Spanish Ministry of Science and Innovation, project number ENE2006-14577-C04-01/FTN. Also, one of us, T.W. performed the work under an Erasmus-Mundus in Nuclear Fusion Science and Engineering Physics scholarship.

References

[1] A. Kirchner et al., Plasma Phys. Control. Fusion 45 (2003) 309.
[2] P.C. Stangeby, J.D. Elder, J. Nucl. Mater. 196–198 (1992) 258.
[3] HYDKIN database, <http://www.eirene.de/eigen/index.html>.
[4] C.S. Pitcher et al., Nucl. Fusion 29 (1989) 1919.
[5] D.G. Whyte et al., Phys. Scripta 111 (2004) 34.
[6] N.H. Brooks et al., J. Nucl. Mater. 363–365 (2007) 131.
[7] For review of methane injection studies for *D/XB* evaluation see: S. Brezinsek et al., J. Nucl. Mater. 363–365 (2007) 1119.
[8] J.D. Strachan et al., Nucl. Fusion 43 (2003) 922.
[9] J. Sanchez et al., J. Nucl. Mater. 390-391 (2009) 852.
[10] A. Hidalgo, D. Tafalla, B. Brañas, F.L. Tabarés, Rev. Sci. Instrum. 75 (2004) 3478.
[11] F.L. Tabarés et al., Plasma Phys. Control. Fusion 43 (2001) 1023.
[12] A.J.R. Heck, R.N. Zare, D.W. Chandler, J. Chem. Phys. 104 (1996) 4019.
[13] K. Behringer et al., J. Nucl. Mater. 176–177 (1990) 606.
[14] U. Fantz et al., J. Nucl. Mater. 337–339 (2005) 1087.
[15] D. Tafalla et al., J. Nucl. Mater. 363–365 (2007) 252.
[16] P. Wienhold et al., J. Nucl. Mater. 290–293 (2001) 362.